

# A photometric redshift of $z = 6.39 \pm 0.12$ for GRB 050904

J. B. Haislip<sup>1</sup>, M. C. Nysewander<sup>1</sup>, D. E. Reichart<sup>1</sup>, A. Levan<sup>2</sup>, N. Tanvir<sup>2</sup>, S. B. Cenko<sup>3</sup>, D. B. Fox<sup>4</sup>, P. A. Price<sup>5</sup>, A. J. Castro-Tirado<sup>6</sup>, J. Gorosabel<sup>6</sup>, C. R. Evans<sup>1</sup>, E. Figueredo<sup>7,8</sup>, C. L. MacLeod<sup>1</sup>, J. R. Kirschbrown<sup>1</sup>, M. Jelinek<sup>6</sup>, S. Guziy<sup>6</sup>, A. de Ugarte Postigo<sup>6</sup>, E. S. Cypriano<sup>8,9</sup>, A. LaCluyze<sup>1</sup>, J. Graham<sup>10</sup>, R. Priddey<sup>2</sup>, R. Chapman<sup>2</sup>, J. Rhoads<sup>11</sup>, A. S. Fruchter<sup>11</sup>, D. Q. Lamb<sup>12</sup>, C. Kouveliotou<sup>13</sup>, R. A. M. J. Wijers<sup>14</sup>, M. B. Bayliss<sup>1,12</sup>, B. P. Schmidt<sup>15</sup>, A. M. Soderberg<sup>3</sup>, S. R. Kulkarni<sup>3</sup>, F. A. Harrison<sup>16</sup>, D. S. Moon<sup>3</sup>, A. Gal-Yam<sup>3</sup>, M. M. Kasliwal<sup>3</sup>, R. Hudec<sup>17</sup>, S. Vitek<sup>18</sup>, P. Kubanek<sup>19</sup>, J. A. Crain<sup>1</sup>, A. C. Foster<sup>1</sup>, J. C. Clemens<sup>1</sup>, J. W. Bartelme<sup>1</sup>, R. Canterna<sup>20</sup>, D. H. Hartmann<sup>21</sup>, A. A. Henden<sup>22</sup>, S. Klose<sup>23</sup>, H.-S. Park<sup>24</sup>, G. G. Williams<sup>25</sup>, E. Rol<sup>26</sup>, P. O'Brien<sup>26</sup>, D. Bersier<sup>27</sup>, F. Prada<sup>6</sup>, S. Pizarro<sup>8</sup>, D. Maturana<sup>8</sup>, P. Ugarte<sup>8</sup>, A. Alvarez<sup>8</sup>, A. J. M. Fernandez<sup>6</sup>, M. J. Jarvis<sup>28</sup>, M. Moles<sup>6</sup>, E. Alfaro<sup>6</sup>, K. M. Ivarsen<sup>1</sup>, N. D. Kumar<sup>1</sup>, C. E. Mack<sup>1</sup>, C. M. Zdarowicz<sup>1</sup>, N. Gehrels<sup>29</sup>, S. Barthelmy<sup>29</sup> & D. N. Burrows<sup>4</sup>

Gamma-ray bursts (GRBs) and their afterglows are the most brilliant transient events in the Universe. Both the bursts themselves and their afterglows have been predicted to be visible out to redshifts of  $z \approx 20$ , and therefore to be powerful probes of the early Universe<sup>1,2</sup>. The burst GRB 000131, at  $z = 4.50$ , was hitherto the most distant such event identified<sup>3</sup>. Here we report the discovery of the bright near-infrared afterglow of GRB 050904 (ref. 4). From our measurements of the near-infrared afterglow, and our failure to detect the optical afterglow, we determine the photometric redshift of the burst to be  $z = 6.39^{+0.11}_{-0.12}$  (refs 5–7). Subsequently, it was measured<sup>8</sup> spectroscopically to be

$z = 6.29 \pm 0.01$ , in agreement with our photometric estimate. These results demonstrate that GRBs can be used to trace the star formation, metallicity, and reionization histories of the early Universe.

At 01:51:44 Universal Time (UT) on 4 September 2005, Swift's Burst Alert Telescope (BAT) detected GRB 050904 and 81 seconds later a 4'-radius localization was distributed to observers on the ground. Swift's X-Ray Telescope (XRT) automatically slewed to the BAT localization and 76 minutes after the burst a 6"-radius XRT localization was distributed.<sup>9</sup>

Over the next few hours, we observed the XRT localization at both



**Figure 1 | NIR and visible-light images of the field of GRB 050904.** Left, NIR discovery image of the bright ( $J = 17.36 \pm 0.04$  mag) afterglow of GRB 050904 from 4.1-m SOAR on top of Cerro Pachon, Chile. Middle, near-simultaneous non-detection of the afterglow at visible wavelengths (unfiltered, calibrated to  $R_c > 20.1$  mag) from one of the six 0.41-m PROMPT telescopes that we are building on top of Cerro Tololo, which is only 10 km away from Cerro Pachon. Right, colour composite ( $r'i'z'$ ) image of the afterglow 3.2 days after the burst from 8.1-m Gemini South, which is also on top of Cerro Pachon.

<sup>1</sup>Department of Physics and Astronomy, University of North Carolina at Chapel Hill, Campus Box 3255, Chapel Hill, North Carolina 27599, USA. <sup>2</sup>Centre for Astrophysics Research, University of Hertfordshire, College Lane, Hatfield AL10 9AB, UK. <sup>3</sup>Department of Astronomy, California Institute of Technology, Pasadena, California 91125, USA. <sup>4</sup>Department of Astronomy and Astrophysics, 525 Davey Laboratory, Pennsylvania State University, University Park, Pennsylvania 16802, USA. <sup>5</sup>Institute for Astronomy, University of Hawaii, 2680 Woodlawn Drive, Honolulu, Hawaii 96822, USA. <sup>6</sup>Instituto de Astrofísica de Andalucía, PO Box 3.004, 18.080 Granada, Spain. <sup>7</sup>Instituto de Astronomia, Geofísica e Ciências Atmosféricas, Universidade de São Paulo, Rua do Matao 1226, 05508-900 São Paulo, SP, Brazil. <sup>8</sup>Southern Observatory for Astrophysical Research, Casilla 603, La Serena, Chile. <sup>9</sup>Laboratorio Nacional de Astrofísica, CP 21, 37500-000 Itajuba, MG, Brazil. <sup>10</sup>Department of Astronomy, 601 Campbell Hall, University of California, Berkeley, California 94720, USA. <sup>11</sup>Space Telescope Science Institute, 3700 San Martin Drive, Baltimore, Maryland 21218, USA. <sup>12</sup>Department of Astronomy and Astrophysics, University of Chicago, Chicago, Illinois 60637, USA. <sup>13</sup>NASA Marshall Space Flight Center, National Space Science Technology Center, 320 Sparkman Drive, Huntsville, Alabama 35805, USA. <sup>14</sup>Astronomical Institute "Anton Pannekoek", University of Amsterdam and Center for High-Energy Astrophysics, Kruislaan 403, 1098 SJ Amsterdam, The Netherlands. <sup>15</sup>Mount Stromlo and Siding Spring Observatories, Private Bag, Weston Creek PO, Canberra, ACT 2611, Australia. <sup>16</sup>Space Radiation Laboratory, California Institute of Technology, MC 220-47, Pasadena, California 91125, USA. <sup>17</sup>Astronomical Institute, Academy of Sciences of the Czech Republic, 25165 Ondřejov, Czech Republic. <sup>18</sup>Faculty of Electrotechnics, Czech Technical University, 121 35 Praha, Czech Republic. <sup>19</sup>Integral Science Data Center, Chemin d'Ecogia 16, CH-1290 Versoix, Switzerland. <sup>20</sup>Department of Physics and Astronomy, University of Wyoming, PO Box 3905, Laramie, Wyoming 82072, USA. <sup>21</sup>Clemson University, Department of Physics and Astronomy, Clemson, South Carolina 29634, USA. <sup>22</sup>American Association of Variable Star Observers, 25 Birch Street, Cambridge, Massachusetts 02138, USA. <sup>23</sup>Thüringer Landessternwarte Tautenburg, Sternwarte 5, D-07778 Tautenburg, Germany. <sup>24</sup>Lawrence Livermore National Laboratory, 7000 East Avenue, Livermore, California 94550, USA. <sup>25</sup>Multiple Mirror Telescope Observatory, University of Arizona, Tucson, Arizona 85721, USA. <sup>26</sup>Department of Physics and Astronomy, University of Leicester, Leicester LE1 7RH, UK. <sup>27</sup>Astrophysics Research Institute, Liverpool John Moores University, Twelve Quays House, Egerton Wharf, Birkenhead CH41 1LD, UK. <sup>28</sup>Astrophysics, Department of Physics, University of Oxford, Keble Road, Oxford OX1 3RH, UK. <sup>29</sup>NASA/Goddard Space Flight Center, Greenbelt, Maryland 20771, USA.

**Table 1 | Observations of the afterglow of GRB 050904**

Date (UT)	Mean $\Delta t$	Filter	Zero point (Jy)	Magnitude*	Telescope
Sep 4.0795	2.80 min	R	3,105	>18.2	0.30-m BOOTES-1B
Sep 4.0821	6.46 min	R	3,105	>18.3	0.30-m BOOTES-1B
Sep 4.0868	13.22 min	R	3,105	>19.2	0.30-m BOOTES-1B
Sep 4.0956	25.95 min	R	3,105	>19.5	0.30-m BOOTES-1B
Sep 4.1151	53.96 min	R	3,105	>19.9	0.30-m BOOTES-1B
Sep 4.1535	109.30 min	R	3,105	>21.0	3.5-m Calar Alto
Sep 4.206	3.07 h	J	1,614	$17.36 \pm 0.04$	4.1-m SOAR
Sep 4.213	3.25 h	J	1,614	$17.35 \pm 0.04$	4.1-m SOAR
Sep 4.220	3.42 h	J	1,614	$17.61 \pm 0.04$	4.1-m SOAR
Sep 4.248	4.08 h	z	3,631	>18.8	60-inch Palomar
Sep 4.355	6.66 h	R	3,105	>22.3	60-inch Palomar
Sep 4.366	6.91 h	Unfiltered, calibrated to $R_c$	3,105	>20.1	0.41-m PROMPT-5
Sep 4.390	7.49 h	J	1,614	$18.66 \pm 0.15$	4.1-m SOAR
Sep 4.402	7.78 h	$K_s$	676	$16.77 \pm 0.07$	4.1-m SOAR
Sep 4.416	8.12 h	i	3,631	>21.1	60-inch Palomar
Sep 4.486	9.79 h	H	1,049	$18.17 \pm 0.06$	3.8-m UKIRT
Sep 4.488	9.86 h	J	1,614	$19.02 \pm 0.06$	3.8-m UKIRT
Sep 4.502	10.18 h	K	676	$17.38 \pm 0.06$	3.8-m UKIRT
Sep 4.518	10.57 h	$K'$	676	$17.55 \pm 0.03$	3.0-m IRTF
Sep 4.551	11.35 h	Z	2,270	$22.08 \pm 0.16$	3.8-m UKIRT
Sep 4.565	11.69 h	J	1,614	$19.25 \pm 0.07$	3.8-m UKIRT
Sep 5.198	26.90 h	Y	2,060	$20.42 \pm 0.26$	4.1-m SOAR
Sep 5.246	28.03 h	J	1,614	$20.16 \pm 0.17$	4.1-m SOAR
Sep 5.322	29.87 h	$l_c$	2,433	>20.2	0.41-m PROMPT-3 + 0.41-m PROMPT-5
Sep 6.30	2.22 day	J	1,614	$20.60 \pm 0.23$	4.1-m SOAR
Sep 6.35	2.27 day	Y	2,060	$20.98 \pm 0.34$	4.1-m SOAR
Sep 7.21	3.13 day	$i'$	3,631	>25.4	8.1-m Gemini South
Sep 7.23	3.15 day	$r'$	3,631	>26.5	8.1-m Gemini South
Sep 7.24	3.16 day	$z'$	3,631	$23.36 \pm 0.14$	8.1-m Gemini South

\* Error bars are  $1\sigma$  and upper limits are  $3\sigma$ .

We calibrated the  $r'z'$  measurements using stellar Sloan Digital Sky Survey (SDSS) sources and derived  $R_c l_c$  field calibrations from the SDSS field calibrations<sup>24</sup>. We obtained YJHK<sub>s</sub>K field calibrations using SOAR and ZJHK field calibrations using UKIRT. The JHK field calibrations are in agreement with each other and with the 2-Micron All-Sky Survey (2MASS). However, the UKIRT Z-band measurement, which we obtained 11.4 h after the burst, is a factor of three below the fitted model (Fig. 2). The UKIRT WFCAM Z bandpass was designed to match the effective wavelength of the SDSS  $z'$  bandpass (0.876 versus 0.887  $\mu\text{m}$ ), but with a rectangular profile. The standard deviation of the magnitude differences for all stellar SDSS sources in the UKIRT Z field and the Gemini South  $z'$  field, which we obtained 3.2 days after the burst, is only 0.064 mag. When converting from magnitudes to spectral fluxes, we used the correct zero points for Z and  $z'$ , respectively. When fitting to these spectral fluxes, we used the actual UKIRT WFCAM Z and Gemini South GMOS-S  $z'$  bandpasses. No modification of the model spectrum (for example, dust extinction<sup>21</sup>, molecular hydrogen absorption<sup>25</sup>, or the Ly $\alpha$  damping wing) appears to be able to accommodate both measurements simultaneously. Consequently, we conclude that this factor-of-three deficit is not only real but probably temporal in nature.

near-infrared (NIR) and visible wavelengths (Table 1). In the NIR, we discovered a bright ( $J \approx 17.4$  mag at 3.1 hours after the burst) and fading source within the XRT localization using the 4.1-m Southern Observatory for Astrophysical Research (SOAR) telescope on top of Cerro Pachon in Chile (Fig. 1).<sup>4</sup>

However, at visible wavelengths we did not detect the afterglow to relatively deep limiting magnitudes using one of the six 0.41-m Panchromatic Robotic Optical Monitoring and Polarimetry Telescopes (PROMPT)<sup>10</sup> that we are building on top of Cerro Tololo, which is only 10 km away from Cerro Pachon<sup>4</sup>, the 60-inch telescope at Palomar Observatory in California<sup>11</sup>, and the 3.5-m telescope at Calar Alto Observatory in Spain. Nor did we detect the afterglow with the 0.30-m Burst Observer and Optical Transient Exploring System (BOOTES)<sup>12</sup> 1B telescope in El Arenosillo, Spain, which began imaging the field only 2.1 minutes after the burst<sup>13</sup>. This implies that the GRB either occurred at a very high redshift or was very heavily extinguished by dust<sup>4</sup>.

Between about 3 hours and about 0.5 days after the burst, the fading of the afterglow appears to be well described by a power law of index  $-1.36^{+0.07}_{-0.06}$  (Fig. 2)<sup>5,6</sup>. However, after this time the fading appears to have slowed to a temporal index of  $-0.82^{+0.21}_{-0.08}$  (refs 7, 14, 15). A single power-law description is ruled out at the  $3.7\sigma$  credible level. One possible explanation is that our initial SOAR observations caught the tail end of a reverse shock that had been stretched in time by a factor of 7.29 owing to cosmological time dilation. Even so, the reverse shock would still be at least a few times longer-lived in the source frame than the reverse shocks of GRBs 990123 and 021211 (refs 16, 17). Another possibility is that we are undersampling a light curve that is undergoing temporal variations, such as in the afterglows of GRBs 021004 and 030329 (refs 18, 19). Indeed, the X-ray afterglow is extremely variable at these times<sup>20</sup>.

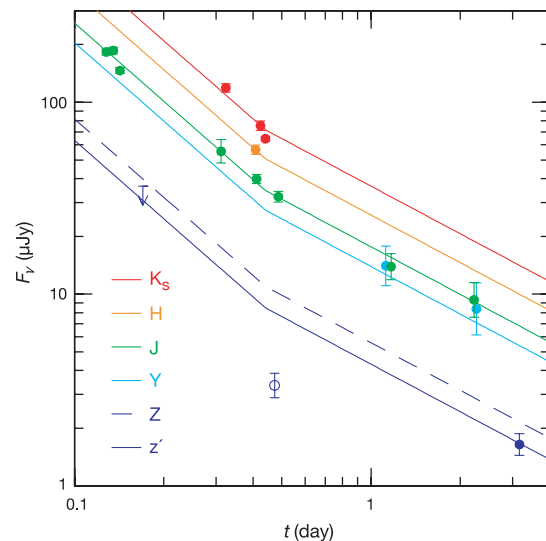


**Figure 2 | NIR and  $z'$ -band light curves of the afterglow of GRB 050904 and our best-fit model.** A single power-law description is ruled out at the  $3.7\sigma$  credible level. Following the formalism of Frail *et al.*<sup>26</sup>, given GRB 050904's redshift and fluence<sup>27</sup> the non-detection of a jet break in the light curve prior to 2.3 days after the burst implies that the opening/viewing angle of the jet is  $\geq 3^\circ$  and that the total energy that was released in  $\gamma$  rays is  $\geq 5 \times 10^{50}$  erg. The Z-band measurement (unfilled circle) is a factor of three below the fitted model, but this appears to be real and temporal in nature (Table 1). Error bars are s.e.m. Downward arrow indicates upper limit.

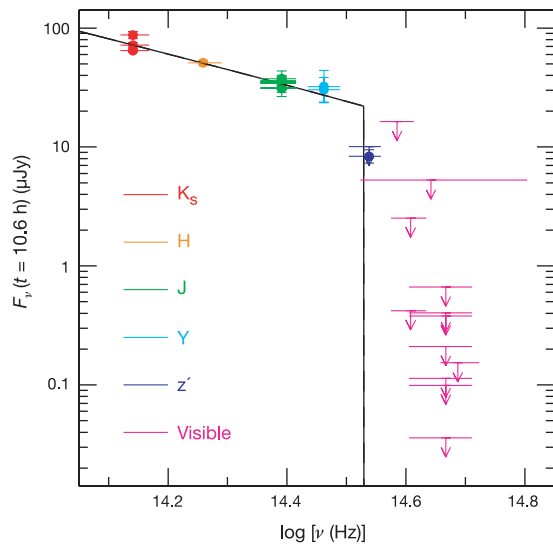


**Figure 3 | Spectral flux distribution of the afterglow of GRB 050904 and our best-fit model.** Measurements have been scaled to 10.6 hours after the burst using our best-fit light curve. We model the spectrum as a power law with negligible emission blueward of  $\text{Ly}\alpha$ . Shallower intrinsic power-law spectra can be inferred with the addition of source-frame dust. If one assumes that the jet is propagating through either a constant-density or wind-swept medium with the synchrotron electron cooling frequency either redward or blueward of the observed frequencies, the fitted temporal index ( $-0.82^{+0.21}_{-0.08}$ ) implies an electron energy distribution index between  $1.43^{+0.28}_{-0.11}$  and  $2.09^{+0.28}_{-0.11}$  and an intrinsic spectral index between  $-0.88^{+0.14}_{-0.05}$  and  $-0.21^{+0.14}_{-0.05}$  (refs 28, 29). This is shallower than the fitted spectral index ( $-1.25^{+0.15}_{-0.14}$ ), which suggests that source-frame dust is probably present. However, only a small amount is required to explain such a difference at these source-frame frequencies. This cannot explain the sharp drop in spectral flux in and blueward of the  $z'$  band<sup>5,21</sup>. We take Galactic  $E(B - V) = 0.060$  mag (ref. 30). Error bars are s.e.m. Downward arrows indicate upper limits.

Using these temporal indices to scale all of our measurements to a common time, except for a Z-band ( $0.84\text{--}0.93\ \mu\text{m}$ ) measurement from 11.4 hours after the burst (Table 1), we plot the spectral flux distribution of the afterglow in Fig. 3. In the NIR, the spectral index is  $-1.25^{+0.15}_{-0.14}$ . However, the spectral index between NIR and visible wavelengths is steeper than  $-5.9$ . This is too sharp a transition to be explained by dust extinction alone<sup>5,21</sup>. However, a small amount of extinction cannot be ruled out and is probably present (Fig. 3).

Assuming negligible emission blueward of  $\text{Ly}\alpha$ , we measure a photometric redshift of  $z = 6.39^{+0.11}_{-0.12}$  (refs 5–7), which is consistent with the spectroscopic redshift of  $z = 6.29 \pm 0.01$  (ref. 8). For  $H_0 = 71\ \text{km s}^{-1}\text{Mpc}^{-1}$ ,  $\Omega_m = 0.27$ , and  $\Omega_\Lambda = 0.73$  (ref. 22), this corresponds to about 900 million years after the Big Bang, when the Universe was about 6% of its current age. The next-most-distant GRB that has been identified occurred at  $z = 4.50$  (ref. 3), which was about 500 million years later, when the Universe was about 10% of its current age.

One of the most exciting aspects of this discovery is the brightness of the afterglow: extrapolating back to a few minutes after the burst, the afterglow must have been exceptionally bright redward of  $\text{Ly}\alpha$  for the robotic 0.25-m TAROT telescope to detect it in unfiltered visible-light observations<sup>23</sup>. Extrapolating our J-band light curve back to these times yields  $J \approx 11\text{--}12$  mag. This suggests that by pairing visible-light robotic telescopes with NIR robotic telescopes, and these with larger telescopes that are capable of quick-response NIR spectroscopy, all preferably at the same site so that they are subject to the same observing conditions, at least some very-high-redshift afterglows will be discovered, identified, and their NIR spectrum

taken while they are still sufficiently bright to serve as a powerful probe of the conditions of the early Universe<sup>10</sup>.

Received 23 September; accepted 12 December 2005.

- Lamb, D. Q. & Reichart, D. E. Gamma-ray bursts as a probe of the very high redshift Universe. *Astrophys. J.* **536**, 1–18 (2000).
- Ciardi, B. & Loeb, A. Expected number and flux distribution of gamma-ray burst afterglows with high redshifts. *Astrophys. J.* **540**, 687–696 (2000).
- Andersen, M. I. *et al.* VLT identification of the optical afterglow of the gamma-ray burst GRB 000131 at  $z = 4.50$ . *Astron. Astrophys.* **364**, L54–L61 (2000).
- Haislip, J. *et al.* GRB 050904: SOAR/PROMPT observations. *GCN Circ.* **3913** (2005).
- Haislip, J. *et al.* GRB 050904: possible high-redshift GRB. *GCN Circ.* **3914** (2005).
- Reichart, D. GRB 050904: environmental constraints. *GCN Circ.* **3915** (2005).
- Haislip, J. *et al.* GRB 050904: SOAR YJ and PROMPT 1c observations. *GCN Circ.* **3919** (2005).
- Kawai, N., Yamada, T., Kosugi, G., Hattori, T. & Aoki, K. GRB 050904: Subaru optical spectroscopy. *GCN Circ.* **3937** (2005).
- Cummings, J. *et al.* GRB050904: Swift-BAT detection of a probable burst. *GCN Circ.* **3910** (2005).
- Reichart, D. *et al.* PROMPT: panchromatic robotic optical monitoring and polarimetry telescopes. *Nuovo Cim.* **28**, 767–770 (2005).
- Fox, D. B. & Cenko, S. B. GRB050904: P60 observations. *GCN Circ.* **3912** (2005).
- Castro-Tirado, A. J. *et al.* Simultaneous and optical follow-up GRB observations by BOOTES. *Nuovo Cim.* **28**, 715–718 (2005).
- Jelinek, M. *et al.* GRB 050904: Bootes early R-band detection. *GCN Circ.* **3929** (2005).
- D'Avanzo, P. *et al.* GRB 050904: NIR object inside the XRT error box. *GCN Circ.* **3921** (2005).
- D'Avanzo, P. *et al.* GRB 050904: more VLT NIR observations. *GCN Circ.* **3930** (2005).
- Akerlof, C. *et al.* Observations of contemporaneous optical radiation from a gamma-ray burst. *Nature* **398**, 400–402 (1999).
- Li, W., Filippenko, A. V., Chornock, R. & Jha, S. The early light curve of the optical afterglow of GRB 021211. *Astrophys. J.* **586**, L9–L12 (2003).
- Fox, D. W. *et al.* Early optical emission from the  $\gamma$ -ray burst of 4 October 2002. *Nature* **422**, 284–286 (2003).
- Price, P. A. *et al.* The bright optical afterglow of the nearby  $\gamma$ -ray burst of 29 March 2003. *Nature* **423**, 844–847 (2003).
- Watson, D. *et al.* Outshining the Quasars at reionization: The X-ray spectrum and lightcurve of the redshift 6.29  $\gamma$ -ray burst GRB 050904. *Astrophys. J.* (submitted).
- Reichart, D. E. Dust extinction curves and  $\text{Ly}\alpha$  forest flux deficits for use in modeling gamma-ray burst afterglows and all other extragalactic point sources. *Astrophys. J.* **553**, 235–253 (2001).
- Spergel, D. N. *et al.* First-year Wilkinson microwave anisotropy probe (WMAP) observations: Determination of cosmological parameters. *Astrophys. J. Suppl. Ser.* **148**, 175–194 (2003).
- Klotz, A., Boer, M. & Atteia, J. L. GRB 050904: TAROT optical measurements. *GCN Circ.* **3917** (2005).
- Smith, J. A. *et al.* The  $u'g'r'i'z'$  standard-star system. *Astron. J.* **123**, 2121–2144 (2002).
- Draine, B. T. Gamma-ray bursts in molecular clouds:  $\text{H}_2$  absorption and fluorescence. *Astrophys. J.* **532**, 273–280 (2000).
- Frail, D. A. *et al.* Beaming in gamma-ray bursts: Evidence for a standard energy reservoir. *Astrophys. J.* **562**, L55–L58 (2001).
- Sakamoto, T. *et al.* GRB 050904 BAT refined analysis of complete data set. *GCN Circ.* **3938** (2005).
- Sari, R., Piran, T. & Narayan, R. Spectra and light curves of gamma-ray burst afterglows. *Astrophys. J.* **497**, L17–L20 (1998).
- Chevalier, R. A. & Li, Z.-Y. Gamma-ray burst environments and progenitors. *Astrophys. J.* **520**, L29–L32 (1999).
- Schlegel, D. J., Finkbeiner, D. P. & Davis, M. Maps of dust infrared emission for use in estimation of reddening and cosmic microwave background radiation foregrounds. *Astrophys. J.* **500**, 525–553 (1998).

**Acknowledgements** D.E.R. gratefully acknowledges support from NSF's MRI, CAREER, PREST and REU programmes, NASA's APRA, Swift GI and IDEAS programmes, and especially L. Goodman and H. Cox. D.E.R. also thanks W. Christiansen, B. Carney, and everyone who has worked to make SOAR a reality over the past 19 years. A.L. and N.T. thank B. Cavanagh and A. Adamson of the JAC for their speedy assistance in acquiring and reducing the UKIRT WFCAM data. A.J.C.-T. thanks INTA and CSIC for their support of BOOTES and AYA (including FEDER funds). R.H. and P.K. acknowledge support from GA AV CR and ESA PECS.

**Author Information** Reprints and permissions information is available at [npg.nature.com/reprintsandpermissions](http://npg.nature.com/reprintsandpermissions). The authors declare no competing financial interests. Correspondence and requests for materials should be addressed to D.E.R. ([reichart@physics.unc.edu](mailto:reichart@physics.unc.edu)).